LAMINAR FORCED CONVECTION HEAT TRANSFER OF A NON-NEWTONIAN FLUID IN A SQUARE DUCT

Ashok R. Chandrupatla* and V. M. K. Sastri†

Indian Institute of Technology, Madras—36, India

Abstract—Numerical solutions for laminar heat transfer of a non-Newtonian fluid in the thermal entrance region of a square duct are presented for three thermal boundary conditions. The power-law model characterises the non-Newtonian behavior. The numerical results show that for each flow behavior index the Nusselt number decreases from a maximum value at the entry plane to a limiting value when both velocity and temperature profiles are fully developed. The results are compared with the available solutions for Newtonian fluid and excellent agreement is found.

NOMENCLATURE

a, half width of square duct;

c_p, specific heat of the fluid at constant pressure;

D_h, hydraulic diameter of the duct, $D_h = 4$ (cross-sectional area)/perimeter;

f_D, "Darcy" or "large" friction factor, $(-dp/dx)_{fd} D_h/(\rho u_m^2/2)$ [dimensionless];

Gz, Graetz number, $Re_a Pr/(x/2D_h)$ [dimensionless];

I_2, dimensionless invariant, defined by equation (4);

i, j, k, indices, indicating positions in X, Y and Z directions respectively;

k, thermal conductivity of fluid;

m, parameter in power law stress strain relationship, consistency index;

n, flow behavior index, parameter in the power law model [dimensionless];

p, fluid static pressure;

Nu, Nusselt number, for fully developed flow, hD_h/k [dimensionless];

$Nu_{x,(\ )}$, local Nusselt number for the thermal entrance region: the second subscript in ( ) designates the associated thermal boundary condition—the local Nusselt number is an average value with respect to perimeter at any given cross section x;

$Nu_{m,T}$, logarithmic mean Nusselt number for ⓉT boundary condition;

Pr, Prandtl number, $\rho c_p u_m a/kRe_a$ [dimensionless];

q', input heat flux per unit length through the walls of one quadrant of the duct;

q'', input heat flux per unit area through the duct wall;

Re_a, Reynolds number based on duct half width, $(\rho a^n u_m^{2-n})/m$ [dimensionless];

Re_D, Reynolds number for the duct based on hydraulic diameter, $(\rho D_h^n u_m^{2-n})/m$ [dimensionless];

S, dimensionless local viscosity, defined by equation (3);

T, dimensionless fluid temperature; $= (t-t_w)/(t_e-t_w)$ for ⓉT boundary condition; $= (t-t_e)/(q'/k)$ for Ⓗ1 boundary condition; $= (t-t_e)/(q''a/k)$ for Ⓗ2 boundary condition;

u, axial fluid velocity in duct;

u_m, average fluid velocity in duct;

U, fluid axial velocity component in the X direction, u/u_m [dimensionless];

x, y, z, rectangular cartesian coordinates;

X, dimensionless axial coordinate, $(x/a)/Re_a$;

X^*, dimensionless axial distance, $X^* = 1/Gz = (x/D_h)/(2Re_a Pr)$;

Y, Z, dimensionless transverse coordinates, $Y = y/a, Z = z/a$;

W, relaxation parameter.

Greek symbols

ρ, fluid density;

μ, $m\left[\left(\dfrac{u}{y}\right)^2 + \left(\dfrac{u}{z}\right)^2\right]^{(n-1)/2}$, local dynamic fluid viscosity coefficient at a point in the square duct;

δ, prefix denoting a difference.

Subscripts

b, bulk mean;

e, initial value at $x = 0$ (at duct entrance);

fd, fully developed laminar flow;

m, mean;

---

*Senior Research Fellow, CSIR, Madras.

†Professor, presently visiting Research Professor at the University of Illinois at Chicago Circle, Chicago, Illinois 60680, U.S.A.

$H1$, referring to $\textcircled{H1}$ boundary
        condition;
$H2$, referring to $\textcircled{H2}$ boundary
        condition;
T,   referring to $\textcircled{T}$ boundary
        condition;
w,   wall.

1. INTRODUCTION

INDUSTRIES in which non-Newtonian fluid behavior is encountered include those dealing with rubber, greases, polymer solutions or melts, pharmaceuticals, paints and biological fluids. An understanding of such non-Newtonian fluid flow behavior will contribute substantially to the solution of a variety of problems. It is important to have a knowledge of the characteristics of the forced convective heat transfer in steady laminar non-Newtonian flow through non-circular ducts to exercise a proper control over the performance of the heat exchanger and to economise the process.

Laminar flow solutions for Newtonian fluids were compiled by Shah and London [1] and Porter [2] in an exhaustive manner. The theoretical laminar flow solutions for heat transfer and flow friction for twenty one straight ducts and four curved ducts were compiled by the former while the latter compiled the laminar flow solutions for Newtonian as well as non-Newtonian fluids with constant and variable fluid properties. While Porter considered a very general problem, the report by Shah and London is much more exhaustive in the more limited area.

For Newtonian laminar heat transfer, Montgomery and Wilbulswas [3] and Lyczkowski et al. [4] solved the thermal entry length problem for the rectangular ducts by using explicit finite difference method. The effects of axial heat conduction, viscous dissipation and the thermal energy sources within the fluid were neglected. Heat-transfer solutions for laminar flow of non-Newtonian fluids in non-circular ducts other than parallel plate geometry [5, 6] are not available in the literature.

In this paper, the forced convective heat-transfer information as a function of the pertinent non-dimensional numbers for three boundary conditions, $\textcircled{T}$, $\textcircled{H1}$ and $\textcircled{H2}$ is presented for the non-Newtonian flow in a square duct.

2. GOVERNING EQUATIONS

The applicable dimensionless momentum and energy equations for the non-Newtonian case with appropriate boundary conditions are outlined below to describe the heat-transfer characteristics through the straight square duct.

Three representative heat-transfer modes as suggested by Irvine [7] for the rectangular channel case are considered. The boundary conditions on the energy equation present a problem for square duct. The three cases considered are:

(1) Constant wall temperature both peripherally and axially; referred to as $\textcircled{T}$ boundary condition.

(2) Constant heat input per unit axial distance and constant peripheral wall temperature at each axial position, with wall temperature varying axially only; referred to as $\textcircled{H1}$ boundary condition.

(3) Constant heat input per unit axial distance and per unit peripheral distance; referred to as $\textcircled{H2}$ boundary condition.

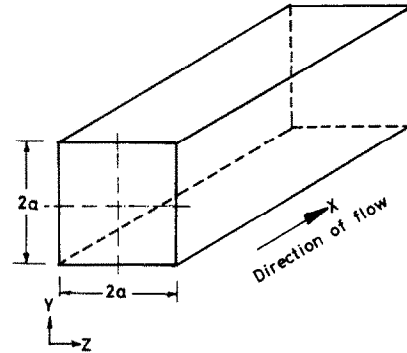The channel configuration and coordinate system are shown in Fig. 1. The origin of the coordinate

FIG. 1. Configuration and coordinate system for square duct.

system is at the bottom left corner of the duct. The application of appropriate symmetry conditions at the cross-section center lines permits the restriction of the solution to one quadrant of the square duct. For the hydrodynamically developed flow, there is only one nonzero component of velocity u, and the constitutive equations of motion reduce to a single nonlinear partial differential equation of the form

$$\frac{\partial}{\partial y}\left(-\mu\frac{\partial u}{\partial y}\right)+\frac{\partial}{\partial z}\left(-\mu\frac{\partial u}{\partial z}\right)+\frac{\mathrm{d}p}{\mathrm{d}x}=0 \qquad (1)$$

where $\mu = m[(\partial u/\partial y)^2+(\partial u/\partial z)^2]^{(n-1)/2}$, local viscosity at a point in the quadrant.

In terms of dimensionless variables and parameters, equation (1) reduces to

$$\frac{\partial}{\partial Y}\left(S\frac{\partial U}{\partial Y}\right)+\frac{\partial}{\partial Z}\left(S\frac{\partial U}{\partial Z}\right)+\frac{f_D Re_D}{2^{n+2}}=0. \qquad (2)$$

The function S is a variable viscosity and is defined in terms of I_2, the second invariant of the irrotational strain-rate tensor. The power law model used in this work to describe the stress strain-rate relation for pseudoplastic fluids is given by

$$S = I_2^{(n-1)/2} \qquad (3)$$

where

$$I_2 = \left(\frac{\partial U}{\partial Y}\right)^2+\left(\frac{\partial U}{\partial Z}\right)^2. \qquad (4)$$

Equation (2) is subject to the boundary condition:

at the walls, $Y = 0$ and $Z = 0$: $U = 0$ $\qquad (5)$

and the constraining equation:

$$\int_0^1\int_0^1 U\,\mathrm{d}Y\,\mathrm{d}Z = 1. \qquad (6)$$

Equation (6) can be regarded as indirectly relating the value of $f_D Re_D$ to the parameter n, the flow behavior index, which appears in the constitutive equation of motion, equation (2).

The dimensionless governing boundary-layer energy equation for constant property flow, neglecting axial conduction and viscous dissipation, is

$$U \frac{\partial T}{\partial X} = \frac{1}{Pr} \left[\frac{\partial^2 T}{\partial Y^2} + \frac{\partial^2 T}{\partial Z^2} \right]. \qquad (7)$$

The boundary condition for Ⓣ , ⒣ and ⒣2 cases are given as follows:

Case 1:

$$T(0, Y, Z) = 1 \qquad (8)$$

$$T(X, 0, Z) = 0 \qquad (9)$$

$$T(X, Y, 0) = 0 \qquad (10)$$

$$\frac{\partial T}{\partial Y}(X, 1, Z) = 0 \qquad (11)$$

$$\frac{\partial T}{\partial Z}(X, Y, 1) = 0. \qquad (12)$$

Case 2:

$$T(0, Y, Z) = 0 \qquad (13)$$

$$\int_0^1 \frac{\partial T}{\partial Z}\bigg|_0 dY + \int_0^1 \frac{\partial T}{\partial Y}\bigg|_0 dZ = 1 \qquad (14)$$

$$\frac{\partial T}{\partial Y}(X, 1, Z) = 0 \qquad (15)$$

$$\frac{\partial T}{\partial Z}(X, Y, 1) = 0. \qquad (16)$$

Case 3:

$$T(0, Y, Z) = 0 \qquad (17)$$

$$\frac{\partial T}{\partial Y}(X, 0, Z) = 1 \qquad (18)$$

$$\frac{\partial T}{\partial Z}(X, Y, 0) = 1 \qquad (19)$$

$$\frac{\partial T}{\partial Y}(X, 1, Z) = 0 \qquad (20)$$

$$\frac{\partial T}{\partial Z}(X, Y, 1) = 0. \qquad (21)$$

3. FINITE-DIFFERENCE REPRESENTATIONS AND METHOD OF SOLUTION

The numerical solution of equation (7) is characterized by the replacement of continuous derivatives by finite difference representations defined at the nodes of a three dimensional rectangular mesh superimposed on one quadrant of a cross-section of the duct.

The indices (i, j, k) indicate positions in the X, Y and Z directions respectively. The origin is designated by $i = j = k = 1$. The axial mesh spacing is h_x. The cross-section center lines, $Y = 1$ and $Z = 1$, are designated by $j = N+1$ and $k = N+1$ respectively. The transverse mesh spacings h_y and h_z are both equal to $1/N$, where N is the number of increments between the wall

and center-line across the quarter duct. The values of U and T are denoted by the following notation. $\beta2(j, k)$ denotes the variable β at a point in the mesh $(i+1, j, k)$ and $\beta1(j, k)$ denotes the variable β at (i, j, k). For example, in $T2(j, k)$, the index j gives the position relative to origin in the Y direction and the second index k gives the position in the Z direction.

The dimensionless fully developed velocity profile, U, for each flow behavior index, n, is obtained from the marching solution described in an earlier paper of the authors [8]. The following finite difference representations are developed with the notation described above.

$$\frac{\partial T}{\partial X} = \frac{T2(j, k) - T1(j, k)}{h_x} \qquad (22)$$

$$\frac{\partial^2 T}{\partial Y^2} = \frac{T2(j+1, k) - 2T2(j, k) + T2(j-1, k)}{h_y^2} \qquad (23)$$

$$\frac{\partial^2 T}{\partial Z^2} = \frac{T2(j, k+1) - 2T2(j, k) + T2(j, k-1)}{h_z^2}. \qquad (24)$$

The finite difference form of energy equation is

$$U2(j, k) \frac{T2(j, k) - T1(j, k)}{h_x}$$

$$= \frac{1}{Pr} \left[\frac{T2(j+1, k) - 2T2(j, k) + T2(j-1, k)}{h_y^2} \right.$$

$$\left. + \frac{T2(j, k+1) - 2T2(j, k) + T2(j, k-1)}{h_z^2} \right]. \qquad (25)$$

The variable $T1$ is known while the variable $T2$ is to be determined at axial position $(i+1)$. The iterative procedure employed is described for each of the thermal boundary conditions. The iterative scheme for the solution of equation (25) is extrapolated Liebmann method. The principal variable for equation (25) at $(i+1, j, k)$ is the axial temperature at that point.

The numerical solution, obtained by using the extrapolated Liebmann method [9] is an iterative procedure requiring initial estimates of the variables at each node. The results from the preceding axial position are substituted as an initial guess for the variables at $(i+1)$ position. The iterative scheme of the principal variable (25) is

$$\overset{(1+1)}{T2(j, k)} = \overset{(1)}{T2(j, k)}$$

$$- W[d_1(\overset{(1)}{T2(j+1, k)} + \overset{(1+1)}{T2(j-1, k)}$$

$$+ \overset{(1)}{T2(j, k+1)} + \overset{(1+1)}{T2(j, k-1)})$$

$$- d_2 \overset{(1)}{T2(j, k)} + d_6] \qquad (26)$$

for $j = 2, 3, \ldots, N+1$

and $k = 2, 3, \ldots, N+1$

where 1 refers to the iteration counter, W is the relaxation parameter, and,

$$d_1 = -h_x/(Pr h_y h_y), \tag{27}$$

$$d_2 = 4d_1 - U2(j, k), \tag{28}$$

and

$$d_3 = -U2(j, k) T1(j, k). \tag{29}$$

Equation (26) is used to solve for each value of $T2(j, k)$ in the field, repeating in some regular order until the values of $T2(j, k)$ on successive iterations agree to within the desired accuracy, equal to, 10^{-6}.

$$\left| \frac{(1+1) \qquad (1)}{T2(j, k) - T2(j, k)} \right| \leqslant 10^{-6}$$

$$\text{for } j = 2, 3, \ldots, N+1, \text{ and}$$

$$k = 2, 3, \ldots, N+1. \tag{30}$$

A step h_x downstream is then taken and the above process is repeated. Convergence of the iterative procedure is obtained by underrelaxation, the relaxation parameter being 0.75.

Stability and rate of convergence are functions of the relaxation parameter, the mesh size (axial as well as transverse), the axial velocity profile and the nature of the estimated temperature profile. The results of the numerical experiments indicate that the finite difference equations of the model are consistent and stable.

(a) Ⓣ Condition

After the dimensionless temperature distribution is obtained, the bulk mean temperature, T_b, the local Nusselt number, $Nu_{x,T}$, and the logarithmic mean Nusselt number, $Nu_{m,T}$, are computed at the axial position in the following way.

$$T_b = \int_0^1 \int_0^1 U T2 \, dY \, dZ. \tag{31}$$

Equation (31) is evaluated using Simpson's Double Integral Rule. Based on the energy balance on the duct length of δx, the local Nusselt number $Nu_{x,T}$ is presented in terms of the fluid bulk mean temperature gradient along the flow length in equation (32).

$$Nu_{x,T} = -(Pr/T_b)(d T_b/dX). \tag{32}$$

The local Nusselt number $Nu_{x,T}$ can also be expressed in terms of temperature gradient at the wall as,

$$Nu_{x,T} = \frac{1}{T_b} \left[\int_0^1 \frac{\partial T}{\partial Y} \Big|_{Y=0} dZ + \int_0^1 \frac{\partial T}{\partial Z} \Big|_{Z=0} dY \right]. \tag{33}$$

The numerical values obtained for $Nu_{x,T}$ from equations (32) and (33) agree excellently up to first four digits.

$$Nu_{m,T} = \frac{Pr}{X} \ln(1/T_b). \tag{34}$$

Even though Prandtl number appears in the dimensionless energy equation explicitly, for all values of

Prandtl number, the thermal entry solution, that is, the variation of predicted mean Nusselt number with Graetz number, obtained is the same. But the effect of Prandtl number is included in the parameter Graetz number which is defined as $Pr/(X/4)$.

(b) Ⓗ Condition

The wall temperature is assumed constant around the perimeter at any given cross-section and to vary only with distance along the duct. At each step of the computation, a new value of wall temperature is computed from the boundary condition of equation (14).

The finite difference form of the boundary condition, equation (14) is explained below. Expressing only the gradients in finite difference form gives

$$\int_0^1 \frac{3T2(j, 1) - 4T2(j, 2) + T2(j, 3)}{2h_z} dY$$

$$+ \int_0^1 \frac{3T2(1, k) - 4T2(2, k) + T2(3, k)}{2h_y} dZ = 1. \tag{35}$$

Now, for Ⓗ boundary condition, by assumption,

$$T2(j, 1) = T2(1, k) = T_w|_{i+1} \tag{36}$$

where T_w is the dimensionless wall temperature.

Rearranging and solving for T_w, and noting that $h_y = h_z$ and symmetry across the diagonal exists,

$$T_w|_{i+1} = \frac{4}{3} \int_0^1 T2(2, k) dZ$$

$$- \frac{1}{3} \int_0^1 T2(3, k) dZ + \frac{h_z}{3}. \tag{37}$$

Note that the wall temperature appears in the integrals. Solving for $T_w|_{i+1}$, using the finite difference form of Simpson's 1/3 rule for integrals, equation (37) reduces to

$$T_w|_{i+1} = \frac{1}{35} + \frac{4}{105} \left[4 \sum_{k=2,4}^{N} T2(2, k) \right.$$

$$+ 2 \sum_{k=3,5}^{N-1} T2(2, k) + T2(2, N+1) \right]$$

$$- \frac{1}{105} \left[4 \sum_{k=2,4}^{N} T2(3, k) \right.$$

$$+ 2 \sum_{k=3,5}^{N-1} T2(3, k) + T2(3, N+1) \right]. \tag{38}$$

After each sweep through the field, the wall temperature T_w is computed using equation (38). Successive sweeps through the cross-section are taken until all values of $T2(j, k)$ change by less than 10^{-6} on two successive iterations. The solution is then considered converged and another h_x step taken downstream.

The peripheral average local Nusselt number $Nu_{x,H1}$ and the mean Nusselt number $Nu_{m,H1}$ are evaluated in the following way.

$$Nu_{x,H1} = \frac{1.0}{(T_w - T_b)} \qquad (39)$$

$$Nu_{m,H1} = \frac{1}{X}\int_0^X Nu_{x,H1}\, dX$$

$$= \frac{h_x}{2}\left[Nu_{x,H1}|_1 + 2\sum_{1=2,3}^i Nu_{x,H1}|_1 \right.$$

$$\left. + Nu_{x,H1}|_{i+1} \right]\left(\frac{1}{X_{i+1}}\right). \qquad (40)$$

(c) $\textcircled{H2}$ *Condition*

The energy equation in finite difference form is given by equation (25). The finite difference forms of the boundary conditions, equations (18) and (19), are explained below. Equation (18) in difference form is expressed as

$$\frac{3T2(1,k) - 4T2(2,k) + T2(3,k)}{2h_y} = 1.0. \qquad (41)$$

Equation (19) in difference form is expressed as

$$\frac{3T2(j,1) - 4T2(j,2) + T2(j,3)}{2h_z} = 1.0. \qquad (42)$$

Equations (41) and (42) are solved for $T2(1,k)$ and $T2(j,1)$ respectively.

$$T2(j,1) = \tfrac{2}{3}h_z + \tfrac{4}{3}T2(j,2) - \tfrac{1}{3}T2(j,3) \qquad (43)$$

$$T2(1,k) = \tfrac{2}{3}h_y + \tfrac{4}{3}T2(2,k) - \tfrac{1}{3}T2(3,k) \qquad (44)$$

$$\text{for } j = 2,3,\dots,N+1$$

$$\text{and } k = 2,3,\dots,N+1.$$

The solution method is now similar to that explained already. The wall temperatures along with the interior temperatures are unknown. The values at axial position i are taken as an initial guess and the equations (43) and (44) are solved along with equation (26). After each sweep through the field, the new wall temperatures are computed from equations (43) and (44). Successive sweeps through the cross-section are taken until all values of $T2(j,k)$ change by less than 10^{-6} on two successive iterations.

The peripheral average wall temperature T_w, the local Nusselt number $Nu_{x,H2}$ and the mean Nusselt number $Nu_{m,H2}$ are evaluated after the solution has converged at each axial step in the following way.

$$T_w = \int_0^1 T2(j,1)\, dY$$

$$= \frac{h_y}{3}\left[T2(1,1) + 4\sum_{k=2,4}^N T2(k,1) \right.$$

$$\left. + \sum_{k=3,5}^{N-1} T2(k,1) + T2(N+1,1) \right] \qquad (45)$$

$$Nu_{x,H2} = \frac{2.0}{(T_w - T_b)} \qquad (46)$$

$$Nu_{m,H2} = \frac{1}{X}\int_0^X Nu_{x,H2}\, dX. \qquad (47)$$

4. RESULTS AND DISCUSSION

Limiting Nusselt numbers

The limiting Nusselt number Nu_T, Nu_{H1} and Nu_{H2} for Newtonian fluids are presented in Table 1 with the results of other investigations.

Table 1. Nu_T, Nu_{H1} and Nu_{H2} for Newtonian fluids—square duct

Investigation	Nu_T	Nu_{H1}	Nu_{H2}
Clark and Kays [10]	2.890	3.630	—
Lyczkowski et al. [4]	2.975	—	3.230
Schmidt and Newell [11]	2.970	3.599	—
Shah and London [1]	2.976	3.608	3.091
Montgomery and Wibulswas [3]	2.650	3.600	—
Present numerical solution	2.975	3.612	3.095

The excellent agreement obtained with the limiting Nusselt numbers for Newtonian fluids [1] for $\textcircled{T}$, $\textcircled{H1}$ and $\textcircled{H2}$ conditions establishes the credentials and validity of the numerical marching technique employed in the present investigation. Further, the accuracy obtained is sufficient to warrant the use of the scheme to attack the thermal entry problems for pseudoplastic fluids also with a high degree of confidence.

For hydrodynamically and thermally developed laminar flow of non-Newtonian fluid in a square duct, the limiting Nusselt numbers Nu_T, Nu_{H1} and Nu_{H2}, when all four walls are transferring heat, are presented in Table 2 for $0.5 \leqslant n \leqslant 1.0$.

Table 2. Nusselt numbers for fully developed velocity and temperature profiles in a square duct for pseudoplastic fluids

Flow behavior index, n	Nu_T	Nu_{H1}	Nu_{H2}
1.0	2.975	3.612	3.095
0.9	2.997	3.648	3.106
0.8	3.030	3.689	3.135
0.75	3.050	3.713	3.152
0.7	3.070	3.741	3.171
0.6	3.120	3.804	3.216
0.5	3.184	3.889	3.274

It is observed from Table 2 that Nu_T for the case $n = 0.5$ is 3.184 and is 7% more than the solution for Newtonian fluids. Similarly, for $n = 0.5$, Nu_{H1} and Nu_{H2} are 7.7 and 5.8% more than the solutions for Newtonian fluids respectively.

For Newtonian fluids, the result for Nu_T is 2.975. This value is 17.6% less than that for $\textcircled{H1}$ condition and 3.9% less than the solution for $\textcircled{H2}$ condition. The result for $\textcircled{H2}$ condition is 14.3% less than the solution for $\textcircled{H1}$ condition.

For $n = 0.5$, the result for Nu_T is 18.1% less than the solution for $\textcircled{H1}$ condition and 2.7% less than that for $\textcircled{H2}$ condition. The result for $\textcircled{H2}$ condition is 15.8% less than the solution for $\textcircled{H1}$ condition. Similar behavior is observed for $0.6 \leqslant n \leqslant 0.9$.
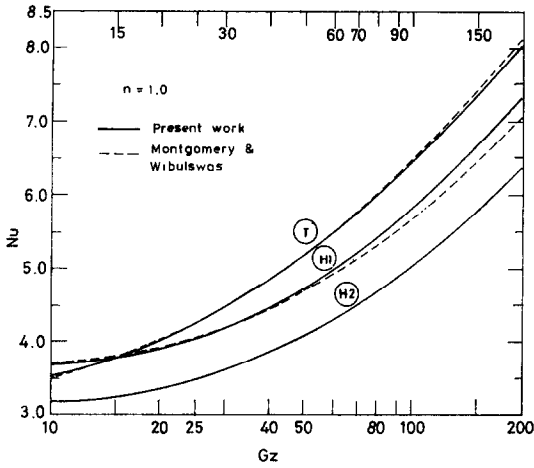
FIG. 2. Square duct—$Nu_{m,T}$, $Nu_{x,H1}$ and $Nu_{x,H2}$ for fully developed velocity profile; $n = 1.0$.
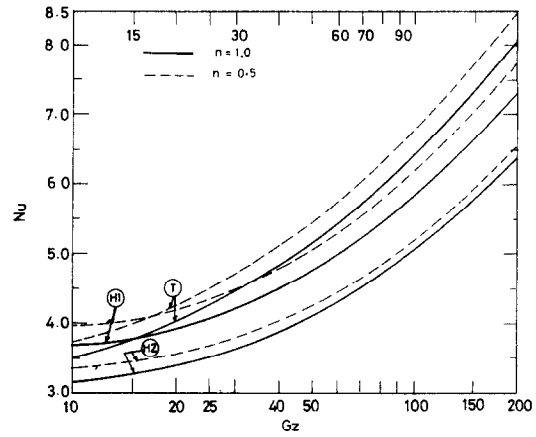

FIG. 3. Square duct—$Nu_{m,T}$, $Nu_{x,H1}$ and $Nu_{x,H2}$ for fully developed velocity profile; $n = 0.5$ and 1.0.

Thermal entry solutions

For hydrodynamically developed flow, the local and mean Nusselt numbers as functions of Graetz number, $0 \leqslant Gz \leqslant 200$, in square duct are presented for $0.5 \leqslant n \leqslant 1.0$ for Ⓣ, Ⓗ and Ⓗ conditions.

$Nu_{m,T}$, $Nu_{x,H1}$ and $Nu_{x,H2}$ as functions of Graetz number are presented in Figs. 2 and 3 for $n = 1.0$ and 0.5 respectively. The numerical results of Montgomery and Wibulswas [3] for Ⓣ and Ⓗ boundary conditions for Newtonian fluid are compared with the present numerical solution in Fig. 2.

The effect of flow behavior index, n, on Nusselt numbers for Ⓣ, Ⓗ and Ⓗ boundary conditions is shown in Fig. 3. The Nusselt number increases with decreasing value of flow behavior index.

(a) Ⓣ *Condition*

$Nu_{x,T}$ and $Nu_{m,T}$ as functions of Graetz number are presented in Tables 3 and 4 respectively for $0.5 \leqslant n \leqslant 1.0$. It is observed from Table 3 that the Nusselt number $Nu_{x,T}$, in the range of 0.5 to 1.0 for the flow

behavior index considered, has a maximum value at the entry plane of the duct and decreases as the Graetz number decreases. $Nu_{x,T}$ approaches the value of the limiting Nusselt number Nu_T, for Graetz number less than 10.

$Nu_{x,T}$ as a function of Graetz number is shown in Fig. 4 and is compared with the results of [3] and [4]. Extremely good agreement is found with the results of Lyczkowski *et al.* [4] for $X^* > 0.075$ and the results are identical for $X^* > 0.09375$. There is an excellent agreement with the numerical results of [3] for $Nu_{x,T}$ and $Nu_{m,T}$ from Graetz number 200 down to 20. However, for $Gz \leqslant 10$, the solution of [3] seems to be diverging rather than attaining a constant and steady value which is not the case in the present solution. Shah and London [1] observed that the results of Lyczkowski *et al.* [4] are more accurate.

(b) Ⓗ *and* Ⓗ *conditions*

$Nu_{x,H1}$, $Nu_{m,H1}$, $Nu_{x,H2}$ and $Nu_{m,H2}$ as functions of Graetz number are presented in Table 5–8 respectively
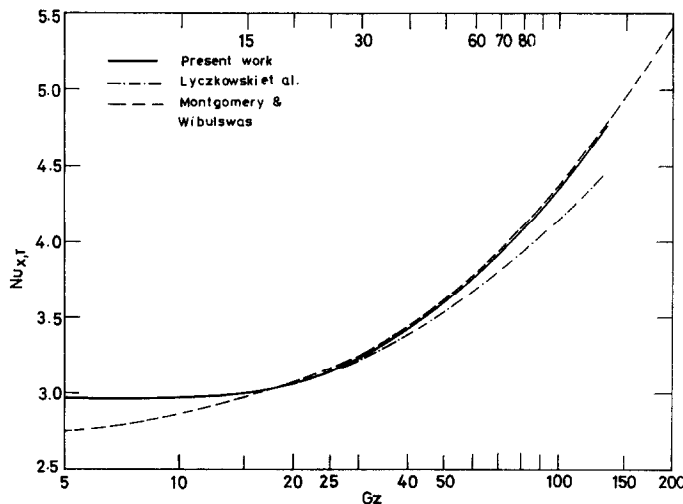

FIG. 4. Square duct—$Nu_{x,T}$ for fully developed velocity profile; $n = 1$.

Table 3. $Nu_{x,T}$ as functions of Gz and n for fully developed velocity profiles

	$Nu_{x,T}$						
	Flow behavior index, n						
Gz	1.0	0.9	0.8	0.75	0.7	0.6	0.5
0	2.975	2.997	3.030	3.050	3.070	3.120	3.184
10	2.976	3.003	3.036	3.055	3.076	3.126	3.189
20	3.074	3.100	3.132	3.151	3.171	3.220	3.283
25	3.157	3.182	3.214	3.233	3.253	3.302	3.365
40	3.432	3.458	3.490	3.510	3.531	3.581	3.646
50	3.611	3.636	3.670	3.690	3.711	3.763	3.830
80	4.084	4.112	4.149	4.170	4.193	4.248	4.321
100	4.357	4.386	4.424	4.446	4.470	4.528	4.604
133.3	4.755	4.787	4.827	4.850	4.876	4.937	5.018
200	5.412	5.448	5.492	5.518	5.546	5.614	5.702

Table 4. $Nu_{m,T}$ as functions of Gz and n for fully developed velocity profiles

	$Nu_{m,T}$						
	Flow behavior index, n						
Gz	1.0	0.9	0.8	0.75	0.7	0.6	0.5
0	2.975	2.997	3.030	3.050	3.070	3.120	3.184
10	3.514	3.543	3.577	3.597	3.619	3.671	3.739
20	4.024	4.055	4.091	4.112	4.135	4.191	4.263
25	4.253	4.284	4.321	4.343	4.367	4.424	4.499
40	4.841	4.877	4.917	4.941	4.967	5.029	5.110
50	5.173	5.211	5.253	5.278	5.305	5.370	5.455
80	5.989	6.033	6.080	6.107	6.137	6.209	6.304
100	6.435	6.483	6.532	6.561	6.592	6.669	6.768
133.3	7.068	7.123	7.175	7.206	7.240	7.322	7.429
200	8.084	8.150	8.208	8.242	8.280	8.370	8.488

Table 5. $Nu_{x,H1}$ as functions of Gz and n for fully developed velocity profiles

	$Nu_{x,H1}$						
	Flow behavior index, n						
Gz	1.0	0.9	0.8	0.75	0.7	0.6	0.5
0	3.612	3.648	3.689	3.713	3.741	3.804	3.889
10	3.686	3.722	3.756	3.789	3.817	3.882	3.968
20	3.907	3.941	3.983	4.007	4.047	4.112	4.182
25	4.048	4.083	4.124	4.149	4.191	4.256	4.325
40	4.465	4.501	4.544	4.569	4.619	4.686	4.753
50	4.720	4.757	4.802	4.828	4.882	4.951	5.017
80	5.387	5.427	5.476	5.504	5.568	5.644	5.711
100	5.769	5.811	5.862	5.892	5.962	6.042	6.109
133.3	6.331	6.376	6.431	6.463	6.550	6.638	6.696
160	6.730	6.778	6.836	6.869	6.952	7.043	7.114
200	7.269	7.320	7.381	7.417	7.507	7.604	7.678

Table 6. $Nu_{m,H1}$ as functions of Gz and n for fully developed velocity profiles

	$Nu_{m,H1}$						
	Flow behavior index, n						
Gz	1.0	0.9	0.8	0.75	0.7	0.6	0.5
0	3.612	3.648	3.689	3.713	3.741	3.804	3.889
10	4.549	4.586	4.610	4.657	4.666	4.735	4.847
20	5.301	5.340	5.388	5.416	5.447	5.522	5.619
25	5.633	5.674	5.723	5.752	5.784	5.861	5.962
40	6.476	6.521	6.575	6.606	6.641	6.725	6.835
50	6.949	6.996	7.052	7.085	7.122	7.210	7.324
80	8.111	8.163	8.225	8.262	8.302	8.399	8.526
100	8.747	8.801	8.867	8.905	8.948	9.050	9.183
133.3	9.653	9.711	9.780	9.822	9.867	9.975	10.117
160	10.279	10.339	10.412	10.454	10.502	10.614	10.761
200	11.103	11.166	11.241	11.286	11.335	11.453	11.607

Table 7. $Nu_{x,H2}$ as functions of Gz and n for fully developed velocity profiles

	$Nu_{x,H2}$						
	Flow behavior index, n						
Gz	1.0	0.9	0.8	0.75	0.7	0.6	0.5
0	3.095	3.106	3.135	3.152	3.171	3.216	3.274
10	3.160	3.185	3.213	3.232	3.252	3.298	3.358
20	3.359	3.382	3.410	3.427	3.445	3.490	3.548
25	3.481	3.504	3.532	3.549	3.567	3.611	3.669
40	3.843	3.866	3.893	3.910	3.928	3.972	4.031
50	4.067	4.089	4.117	4.133	4.152	4.196	4.255
80	4.654	4.677	4.704	4.721	4.740	4.785	4.846
100	4.993	5.015	5.043	5.060	5.078	5.124	5.187
133.3	5.492	5.514	5.542	5.559	5.578	5.625	5.688
160	5.848	5.870	5.898	5.915	5.934	5.981	6.046
200	6.330	6.352	6.379	6.396	6.415	6.463	6.529

Table 8. $Nu_{m,H2}$ as functions of Gz and n for fully developed velocity profiles

	$Nu_{m,H2}$						
	Flow behavior index, n						
Gz	1.0	0.9	0.8	0.75	0.7	0.6	0.5
0	3.095	3.106	3.135	3.152	3.171	3.216	3.274
10	3.915	3.938	3.965	3.982	4.000	4.045	4.104
20	4.602	4.623	4.650	4.667	4.685	4.729	4.788
25	4.898	4.920	4.946	4.963	4.980	5.024	5.084
40	5.656	5.676	5.702	5.718	5.736	5.780	5.840
50	6.083	6.103	6.128	6.144	6.162	6.206	6.266
80	7.138	7.157	7.181	7.196	7.213	7.257	7.318
100	7.719	7.737	7.760	7.775	7.792	7.835	7.895
133.3	8.551	8.567	8.589	8.603	8.619	8.661	8.721
160	9.128	9.143	9.164	9.178	9.193	9.234	9.293
200	9.891	9.905	9.924	9.937	9.951	9.980	10.048

for $0.5 \leqslant n \leqslant 1.0$. The observations made in the case of Ⓣ condition hold good in these cases.

It is observed from Fig. 2 that the present numerical solution $Nu_{x,H1}$ is consistently higher than that presented in [3]. This difference is due to the different numerical schemes adopted. Specifically, Montgomery and Wibulswas [3] used a different procedure for evaluating the wall temperatures. For the same reason, the $Nu_{m,H1}$ are also higher than the results of [3].

5. CONCLUSIONS

In this paper numerical solutions are obtained for laminar flow forced convection heat transfer of pseudoplastic fluid in the thermal entrance region of a square duct for (a) constant and uniform wall temperature peripherally as well as axially, (b) constant axial wall heat flux with uniform peripheral wall temperature and (c) constant axial wall heat flux with uniform peripheral wall heat flux.

The extrapolated Liebmann method is used for the iterative scheme to obtain the numerical solutions. The numerical solution for Newtonian fluid gives values of the limiting Nusselt numbers which agree excellently with those calculated by others [1, 11]. This indicates that the finite difference method employed here is accurate and effective.

From a comparison of the numerical solutions it is concluded that for the same Graetz number and thermal boundary conditions a non-Newtonian fluid with flow behavior index less than one gives a higher heat-transfer coefficient than a Newtonian fluid. The laminar heat-transfer solutions can be used as a lower limit in design since experimental values of the heat-transfer coefficients, generally, are higher than the predicted ones.

Due to reduction in friction power requirement [8] and the increase in heat-transfer rates, pseudoplastic fluids seem to be better working fluids in heat exchange equipment compared to Newtonian fluids.

REFERENCES

1. R. K. Shah and A. L. London, Laminar flow forced convection heat transfer and flow friction in straight and curved ducts—a summary of analytical solutions, T.R. No. 75, Dept. of Mech. Engng, Stanford Univ., Stanford, California (1971).
2. J. E. Porter, Heat transfer at low Reynolds number (highly viscous liquids in laminar flow), *Trans. Instn Chem. Engrs* **49**, 1–29 (1971).
3. S. R. Montgomery and P. Wibulswas, Laminar flow heat transfer in ducts of rectangular cross-section, in *Proceedings of the Third International Heat Transfer Conference*, Vol. 1, pp. 85–98. A.I.Ch.E., New York (1966).
4. R. W. Lyczkowski, C. W. Solbrig and D. Gidaspow, Forced convective heat transfer in rectangular ducts—general case of wall resistances and peripheral conduction, Institute of Gas Technology, Tech. Info. Center, File 3229, 3424 S. State Street, Chicago, Illinois 60616 (1969).
5. J. Yau and C. Tien, Simultaneous development of velocity and temperature profiles for laminar flow of non-Newtonian fluid in the entrance of region of flat ducts, *Can. J. Chem. Engng* **12**, 139–145 (1963).
6. A. R. Chandrupatla and V. M. K. Sastri, Heat transfer in laminar flow of power law, pseudoplastic fluid in entrance region between parallel plates, Presented at the Third National Heat and Mass Transfer Conference, Indian Institute of Technology, Bombay, India (11–13 December 1975).
7. T. F. Irvine, Jr., Non-circular duct convective heat transfer, in *Modern Developments in Heat Transfer*, pp. 1–17. Academic Press, New York (1963).
8. A. R. Chandrupatla and V. M. K. Sastri, Laminar entrance flow of pseudoplastic fluid in a square duct, in The Fifth All Union Heat and Mass Transfer Conference, Minsk, U.S.S.R. (17–20 May 1976).
9. D. W. Peaceman, Lecture notes on numerical solution of elliptic and parabolic partial differential equations. University of Colorado, Boulder, Colorado (1966).
10. S. H. Clark and W. M. Kays, Laminar-flow forced convection in rectangular tubes, *Trans. Am. Soc. Mech. Engrs* **75**, 859–866 (1955).
11. F. W. Schmidt and M. E. Newell, Heat transfer in fully developed laminar flow through rectangular and isosceles triangular ducts, *Int. J. Heat Mass Transfer* **10**, 1121–1123 (1967).

CONVECTION THERMIQUE, FORCEE ET LAMINAIRE, POUR UN FLUIDE NON NEWTONIEN DANS UN CONDUIT CARRE

Résumé—On présente les solutions numériques pour le transfert thermique laminaire d'un fluide non newtonien dans la région d'entrée d'un tube carré, pour trois conditions aux limites thermiques. Le modèle en loi puissance caractérise le comportement non newtonien. Les résultats numériques montrent que pour chaque indice de comportement, le nombre de Nusselt décroît, depuis une valeur maximale à la section d'entrée, jusqu'à une valeur limite quand les profils de vitesse et de température sont tous deux établis. Les résultats sont comparés avec les solutions connues pour les fluides newtoniens et on trouve un accord excellent.

DER WÄRMEÜBERGANG EINES NICHT-NEWTONSCHEN FLUIDES BEI ERZWUNGENER LAMINARER KONVEKTION IN EINEM KANAL MIT QUADRATISCHEM QUERSCHNITT

Zusammenfassung—Für den Wärmeübergang eines nicht-newtonschen Fluides bei laminarer Strömung im Einlaufbereich eines Kanals mit quadratischem Querschnitt werden für drei thermische Randbedingungen numerische Lösungen angegeben. Das nicht-newtonsche Verhalten wird durch ein Potenzgesetz beschrieben. Für jeden Strömungsfall zeigen die numerischen Ergebnisse einen Abfall der Nusselt-Zahl vom Maximalwert in der Einlaufebene auf einen Grenzwert bei voll ausgebildeten Geschwindigkeits- und Temperaturprofilen. Die Ergebnisse werden mit vorhandenen Lösungen für newtonsche Fluide verglichen; dabei ergibt sich eine ausgezeichnete Übereinstimmung.

ТЕПЛООБМЕН НЕНЬЮТОНОВСКОЙ ЖИДКОСТИ В КАНАЛЕ КВАДРАТНОГО СЕЧЕНИЯ ПРИ ВЫНУЖДЕННОЙ КОНВЕКЦИИ В ЛАМИНАРНОМ ПОТОКЕ

Аннотация — Представлены численные решения задачи теплообмена при ламинарном течении неньютоновской жидкости на тепловом начальном участке канала прямоугольного сечения для трех типов тепловых граничных условий. Неньютоновское поведение среды охарактеризовано степенной моделью. Численные результаты показывают, что для каждого значения индекса неньютоновости число Нуссельта уменьшается от максимальной величины на входе до некоторого предельного значения при полностью развитых профилях скорости и температуры. Сравнение полученных результатов с имеющимися решениями для неньютоновских жидкостей показало хорошее соответствие между ними.